PHOTON PRODUCTION IN RELATIVISTIC NUCLEAR COLLISIONS AT SPS AND RHIC ENERGIES

SIMON TURBIDE[1][*], RALF RAPP[2], AND CHARLES GALE[1]

[1] *Department of Physics, McGill University, 3600 University Street*
Montreal, QC, H3A 2T8 Canada
[2] *Cyclotron Institute and Physics Department, Texas A&M University*
College Station, TX, 77843-3366 USA

Chiral Lagrangians are used to compute the production rate of photons from the hadronic phase of relativistic nuclear collisions. Special attention is paid to the role of the pseudovector a_1 meson. Calculations that include reactions with strange mesons, hadronic form factors and vector spectral densities consistent with dilepton production, as well as the emission from a quark-gluon plasma and primordial nucleon-nucleon collisions, reproduce the photon spectra measured at the Super Proton Synchrotron (SPS). Predictions for the Relativistic Heavy Ion Collider (RHIC) are made.

1. Introduction

The electromagnetic radiation emitted during relativistic heavy ion collisions has been an intense subject of research for several years. As real and virtual photons essentially do not suffer final state interactions, they are good probes of the local condition in the hot matter created. One of the goals of this research program is to investigate whether a new phase of matter (generically called a Quark-Gluon Plasma (QGP)) is formed in nuclear collisions. The existence of this state is a prediction of Quantum Chromodynamics (QCD). However, the measured photons cannot be tagged individually according to their emission phase, and the QGP contribution therefore cannot be isolated in a direct fashion. In order to compare with data, one needs to compute the production rate of photons from the QGP phase, but also from the reactions occurring after hadronization, and from a potential mixed phase. A previous study [1] has shown a comparable bright-

2

ness of partonic and hadronic phases. Later works [2,3] have highlighted the important role played by the a_1 pseudovector meson in the hadronized, non-perturbative sector. Here, we reconsider the axial vector together with constraints imposed by known hadronic phenomenology. We discuss the role of form factors, of the QGP and of the Cronin effffect in primordial nucleon-nucleon collisions in the interpretation of the WA98 photon data, measured at the CERN SPS. Predictions for RHIC will also be shown.

2. Hadronic phase

2.1. *Massive Yang-Mills approach*

The interactions of hadrons can be described by Lagrangians which should respect the fundamental symmetries of QCD. The introduction of vector mesons within the Massive Yang-Mills (MYM) approach provides an adequate meson phenomenology. A chiral $U(3)_L \times U(3)_R$ MYM Lagrangian can be written as[3,4]:

$$
\begin{aligned}
L = &\tfrac{1}{8}F_\pi^2 \mathrm{Tr} D_\mu U D^\mu U^\dagger + \tfrac{1}{8}F_\pi^2 \mathrm{Tr} M(U + U^\dagger - 2) \\
&- \tfrac{1}{2}\mathrm{Tr}\left(F_{\mu\nu}^L F^{L\mu\nu} + F_{\mu\nu}^R F^{R\mu\nu}\right) + m_0^2 \mathrm{Tr}\left(A_\mu^L A^{L\mu\nu} + A_\mu^R A^{R\mu}\right) + \\
&\gamma \mathrm{Tr} F_{\mu\nu}^L U F^{R\mu\nu} U^\dagger - i\xi \mathrm{Tr}\left(D_\mu U D_\nu U^\dagger F^{L\mu\nu} + D_\mu U^\dagger D_\nu U F^{R\mu\nu}\right) \ .
\end{aligned} \quad (1)
$$

In the above,

$$
\begin{aligned}
U &= \exp\left(\frac{2i}{F_\pi}\sum_i \frac{\phi_i \lambda_i}{\sqrt{2}}\right) = \exp\left(\frac{2i}{F_\pi}\phi\right) \ , \\
A_\mu^L &= \tfrac{1}{2}(V_\mu + A_\mu) \ , \\
A_\mu^R &= \tfrac{1}{2}(V_\mu - A_\mu) \ , \\
F_{\mu\nu}^{L,R} &= \partial_\mu A_\nu^{L,R} - \partial_\nu A_\mu^{L,R} - ig_0\left[A_\mu^{L,R}, A_\nu^{L,R}\right] \ , \\
D_\mu U &= \partial_\mu U - ig_0 A_\mu^L U + ig_0 U A_\mu^R \ , \\
M &= \frac{2}{3}\left[m_K^2 + \frac{1}{2}m_\pi^2\right] - \frac{2}{\sqrt{3}}(m_K^2 - m_\pi^2)\lambda_8 \ .
\end{aligned} \quad (2)
$$

The vector and axial vector mesons are included in the theory as gauge bosons. The electromagnetic field is implemented through a U(1) transformation, which leads to the well-known[5] vector-meson-dominance (VMD):

$$
L_{em} = -C m_\rho^2 \rho_\mu^0 B^\mu \ . \quad (3)
$$

This theory leaves 5 unknown parameters $(C, m_0, g_0, \gamma, \xi)$ that we can fit using measured values of $\Gamma_{\rho \to e^- e^+}$, m_ρ, m_{a_1}, $\Gamma_{\rho \to \pi\pi}$, $\Gamma_{a_1 \to \rho\pi}$. This

procedure still allows for two possible sets of solution,

$$(I): \quad \tilde{g} = 10.3063, \ \gamma = 0.3405, \ \xi = 0.4473, \ m_0 = 0.6253 \ \text{GeV} \ ;$$

$$(II): \quad \tilde{g} = 6.4483, \ \gamma = -0.2913, \ \xi = 0.0585, \ m_0 = 0.875 \ \text{GeV} \ , \quad (4)$$

where $\tilde{g} = g_0/\sqrt{1-\gamma}$. To discriminate between the two sets, one can take advantage of another hadronic measurement, the D- to S-wave ratio in the final state of $a_1 \rightarrow \rho\pi$. In addition, the radiative decay width of the a_1 is known experimentally, albeit with somewhat less precision. Note also that as mesons are not fundamental fields, form factors need to be included in the theoretical estimates. This turns out to be especially important in the evaluation of strong off-shell vertices like the one contained in $\Gamma_{a_1 \rightarrow \pi\gamma}$[6]. An evaluation of the D/S ratio and of the radiative decay width yields

$$(I): \ D/S = 0.36, \ \Gamma_{a_1 \rightarrow \pi+\gamma} = 2.2 \ \text{MeV}$$

$$(II): \ D/S = -0.099, \ \Gamma_{a_1 \rightarrow \pi+\gamma} = 0.033 \ \text{MeV} \ . \quad (5)$$

The results with set II agree well with the experimental D/S value of -0.107 ± 0.016. However, neither set I nor set II reproduces the experimental radiative decay width, $\Gamma_{a_1 \rightarrow \pi\gamma} = 0.64 \pm 0.246$ MeV. For the sake of quantitative analysis, we define a third set as

$$(III): \quad \tilde{g} = 5.834, \ \gamma = -0.464, \ \xi = 0.1157, \ m_0 = 0.847 \ \text{GeV} \ , \quad (6)$$

leading to

$$m_{a_1} = 1.4 \ \text{GeV}, \ m_\rho = 0.7 \ \text{GeV}, \ \Gamma_\rho = 0.17 \ \text{GeV} \quad (7)$$

$$\Gamma_{a_1} = 0.3 \ \text{GeV}, \ D/S = -0.49, \ \Gamma_{a_1 \rightarrow \pi+\gamma} = 0.44 \ \text{MeV} \ . \quad (8)$$

2.2. *Photon production rates*

2.2.1. *The role of the a_1 pseudovector*

The photon production rate from hadronic matter is evaluated in relativistic kinetic theory [1,3],

$$q_0 \frac{dR_\gamma}{d^3q} = \int \frac{d^3p_1}{2(2\pi)^3 E_1} \frac{d^3p_2}{2(2\pi)^3 E_2} \frac{d^3p_3}{2(2\pi)^3 E_3} (2\pi)^4 \delta^{(4)}(p_1 + p_2 - p_3 - q)$$

$$\times |M_{12 \rightarrow 3\gamma}|^2 \frac{f(E_1)f(E_2)[1 \pm f(E_3)]}{2(2\pi)^3} \ , \quad (9)$$

where $M_{12 \rightarrow 3\gamma}$ is the process amplitude and f is a Bose-Einstein distribution function. Figure 1 shows the reaction $\pi + \rho \rightarrow \pi + \gamma$ for the three
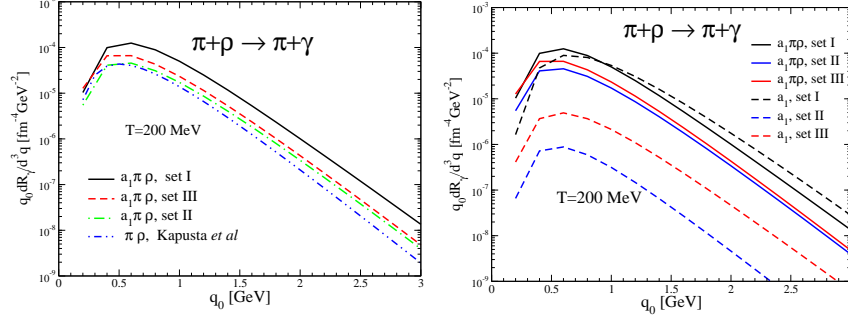
4

Figure 1.   Left panel: $\pi + \rho \to \pi + \gamma$ from $\pi\rho a_1$ intermediate states added coherently, at a temperature of T=200 MeV for the three sets discussed in section I. The dash-double-dotted curve represents the result from Ref. [1]. Right panel: a_1 and $a_1\pi\rho$ contribution to $\pi + \rho \to \pi + \gamma$. No form factors are included here, see next subsection.

sets of parameters. The ordering of those rates is the same as the ordering of a_1 radiative decays: larger radiative decay gives larger results for $\pi + \rho \to \pi + \gamma$. Importantly, we point out that a n-times larger radiative decay does **not** imply the $\pi + \rho \to \pi + \gamma$ rate to be larger by the same factor. This statement is accurate for the pure a_1 contribution to $\pi + \rho \to \pi + \gamma$ (right panel of Fig. 1), but the total $\pi + \rho \to \pi + \gamma$ rate is given by a coherent sum of diagrams containing virtual a_1 and other meson species. Therefore, even if the photon yield from the a_1 diagrams with set I is considerably larger than the corresponding contribution of set II (right panel Fig. 1), the result for set I becomes about four times larger than the result of set II, once we coherently add the other contributions. Note that set II, which reproduces the hadronic phenomenology of the a_1 well, might be considered as a conservative estimate for the contributions of $\pi + \rho \to \pi + \gamma$, as it under-predicts the radiative decay. To quantify this further, we adjusted parameters to reproduce the a_1 electromagnetic width (set III), yielding a photon rate for $\pi + \rho \to \pi + \gamma$ which is larger than that of set II by a factor of less than two. To have a rough estimate of the error associated with those rates, one can simply consider the range spanned by the results of set II (good D/S, wrong $\Gamma_{a_1 \to \pi + \gamma}$) and those of set III (wrong D/S, good $\Gamma_{a_1 \to \pi + \gamma}$). The consequence of this exercise is that set II is used here, and that we regard its inherent uncertainty to be within a factor of two. Note also that the MYM approach, being based on chiral $U(3)_L \times U(3)_R$ symmetry, treats the interaction of non-strange mesons with strange mesons in a coherent way. This is a desirable feature. For the sake of comparison, around E_γ=3 GeV, the result from set II is a

factor 2 larger than that of Ref. [1], where the a_1 was not included.

2.2.2. *Form-factors and the strange sector*

A conventional way to account for the finite size of mesons when using effective models at high momentum transfer is to introduce form factors. To be consistent with the procedure adopted before for dilepton production [6], we assume a standard dipole form for each hadronic vertex appearing in the amplitudes,

$$F(t) = \left(\frac{2\Lambda^2}{2\Lambda^2 - t} \right)^2 \ , \tag{10}$$

using a typical hadronic cutoff scale, $\Lambda = 1$ GeV [6]. We then approximate the four-momentum transfer in a given t-channel exchange of meson X by its average $\bar{t}$ according to [10]

$$\left(\frac{1}{m_X^2 - \bar{t}} \right)^2 \left(\frac{2\Lambda^2}{2\Lambda^2 - \bar{t}} \right)^8 = \frac{1}{4E^2} \int_0^{4E^2} \frac{dt(2\Lambda^2)^8}{(m_X^2 - t)^2(2\Lambda^2 - t)^8} \ . \tag{11}$$

This procedure allows to factorize form factors from amplitudes which facilitates the task of making the final expression gauge invariant. Finally, using the MYM Lagrangian and the above form factor, we calculate amplitudes for all possible (Born-) graphs for the reactions: $X + Y \rightarrow Z + \gamma$, $\rho \rightarrow Y + Z + \gamma$ and $K^* \rightarrow Y + Z + \gamma$. For X, Y, Z every allowed combination of ρ, π, K^*, K mesons was considered. The results for the strange and non-strange sectors are summarized in Fig. 2. Overall, the total strange contribution accounts for $\sim 25\%$ of the net contribution around q_0=1 GeV, while this reduces to $\sim 15\%$ at q_0=3 GeV (right panel of Fig. 2). Parametrizations for all of those reactions are given in Ref. [10]. It is of interest to point out that the rates of Fig. 2 contain a contribution of an ω t-channel exchange, in the case of $\pi\rho$ initial state. This process has been found to contribute significantly, especially if the hadronic couplings are deduced from fits including hadronic form factors, as they should[10].

3. Other sources of photons in Heavy Ions Collisions

We added baryonic sources to the mesonic contribution of the previous section by evaluating in-medium vector spectral functions [7] at the photon point. An important consistency requirement is that the spectral density used for photons needs to be the same as that employed for the interpretation of dilepton measurements [8]. This requirement is fulfilled here, and
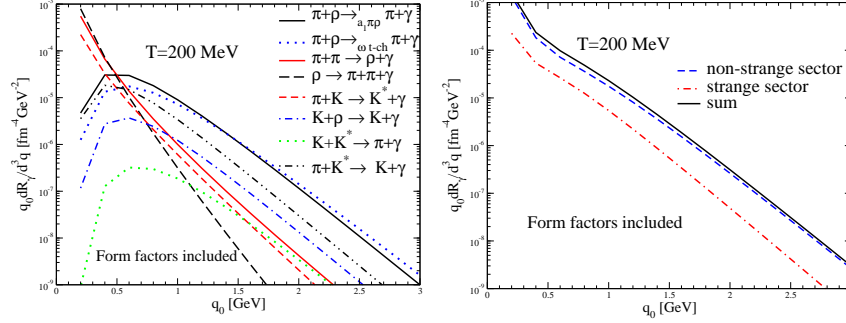
6

Figure 2.   Strange and non-strange meson contributions to the production rate of photons at T=200 MeV.

double-counting issues have received careful consideration. In the case of dilepton production [8,9], baryons have been found to be important sources of virtual photons. In the photon sector, they manifest themselves in the low energy spectrum [10], $q_0 < 1$ GeV. For the production of photons from the quark-gluon plasma, we used the parametrized results of Ref. [11], which include the Laudau-Pomeranchuk-Migdal (LPM) effect [14,15] through a complete leading-order calculation [12,13].

Finally, primordial nucleon-nucleon (N-N) collisions also contribute to the production of direct photons; the pertinent spectra are given by [16]

$$q_0 \frac{dN_\gamma^{prompt}}{d^3q} = q_0 \frac{d^3\sigma_\gamma^{pp}}{d^3q} \frac{N_{coll}}{\sigma_{pp}^{in}} . \tag{12}$$

N_{coll} is the number of N-N collisions, σ_{pp}^{in} is the total inelastic N-N cross-section and $q_0 \frac{d^3\sigma_\gamma^{pp}}{d^3q}$ the differential cross-section to produce photons, which includes intrinsic k_T effects at the N-N level [10,17]. An additional broadening, attributable to the Cronin effect [18], is obtained by folding over a Gaussian transverse momentum distribution [10,19]:

$$f(k_T) = \frac{1}{\pi \langle \Delta k_T^2 \rangle} \, e^{-k_T^2/\langle \Delta k_T^2 \rangle} . \tag{13}$$

The amount of broadening has been estimated by fitting p-A data, and extrapolating to A-A collisions [10]. One then obtains $\langle \Delta k_T^2 \rangle \sim 0.2\text{-}0.3 \, \text{GeV}^2$.

4. Comparison with experiment and predictions

Our total photon production from QGP and hadronic phase is a convolution of the production rate of the previous sections with a fireball evolution

model [7,20] adjusted to reproduce observed flow velocities and hadron ratios. On top of this, we add the photon yield from primordial N-N collisions. With an initial temperature of $T_i = 205$ MeV, our results (left panel Fig. 3) are consistent with WA98 data [21] over the entire spectrum. The high and low q_t regions are dominated by primordial N-N collisions and hadronic phase, respectively. The QGP appears to be sub-dominant over all of the energy range. However, our results for RHIC (right panel of Fig. 3) show that there is a window, 1 GeV $< q_t <$ 3 GeV, through which the QGP shines. The Cronin effect has been neglected for RHIC, as it is expected to be less important than at the SPS [19,22].
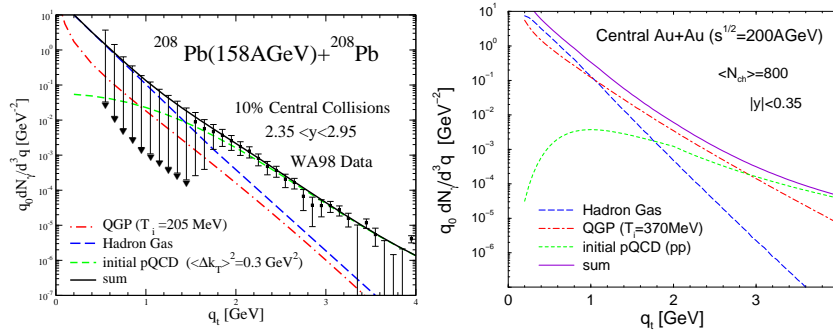

Figure 3.   Left panel: thermal plus prompt photon spectra compared to data from WA98 [21] for central Pb+Pb collisions at SPS. Right panel: photon spectra at RHIC.

5. CONCLUSIONS

We have shown results for the production rate of real photons calculated within a chiral Lagrangian based on a Massive Yang-Mills approach. The pertinent hadronic rate was supplemented by the leading order QCD calculation for QGP to evaluate spectra in central Pb-Pb collisions at SPS using a thermal fireball evolution model. WA98 data are reasonably well reproduced once primordial N-N collisions are also included with a Cronin effect estimated from p-A data. Strange particles are found to have a non-negligible contribution to the photon production rate, $\sim$ 15-25 % of the total hadronic contribution. The QGP contribution is found to be around $\sim$ 20-30% of the thermal yield, implying that the WA98 data can be interpreted, to a large extent, within a hadronic framework. At RHIC, the QGP contribution becomes dominant for intermediate photon energies of

8

around 2 GeV, which provides a promising prospect for the measurement of electromagnetic radiation from relativistic nuclear collisions.

Acknowledgments

References

1. J. Kapusta, P. Lichard and D. Seibert, Phys. Rev. **D44**, 2774 (1991) [erratum-*ibid.* **D47**, 4171 (1991)].
2. L. Xiong, E. Shuryak and G.E. Brown, Phys. Rev. **D46**, 3798 (1992).
3. C. Song, Phys. Rev. **C47**, 2861 (1993).
4. H. Gomm, Ö. Kaymakcalan, and J. Schechter, Phys. Rev. **D30**, 2345 (1984).
5. J. J. Sakurai, *Currents and Mesons*, University of Chicago Press, Chicago (1969).
6. R. Rapp and C. Gale, Phys. Rev. **C60**, 024903 (1999).
7. R. Rapp and J. Wambach, Eur. Phys. J. **A6**, 415 (1999).
8. R. Rapp and J. Wambach, Adv. Nucl. Phys. **25**, 1 (2000).
9. R. Rapp, Pramana **60**, 675 (2003).
10. S. Turbide, R. Rapp and C. Gale, Phys. Rev. **C69**, 014903 (2004).
11. P. Arnold, G. D. Moore and L. G. Yaffe, J. High Energy Phys. **0112**, 9 (2001).
12. P. Arnold, G. D. Moore and L. G. Yaffe, J. High Energy Phys. **0111**, 057 (2001).
13. P. Arnold, G. D. Moore and L. G. Yaffe, J. High Energy Phys. **0206**, 030 (2002).
14. L.D. Landau and I.Pomeranchuk, Dokl. Akad. Nauk S.S.S.R. **92**, 535 (1953); Dokl. Akad. Nauk S.S.S.R. **92**, 735 (1953).
15. A.B. Migdal, Dokl. Akad. Nauk S.S.S.R **105**, 77 (1955); Phys. Rev. **103**, 1811 (1956).
16. C.Y. Wong and H. Wang, Phys. Rev **C58**, 376 (1998).
17. D. K. Srivastava, Eur. Phys. J. C **22**, 129 (2001).
18. J.W. Cronin, H.J. Frisch, M.J. Shochet, J.P. Boymond, R. Mermod, P.A. Piroue, and R.L. Summer, Phys. Rev. D **11**, 3105 (1975).
19. A. Dumitru, L. Frankfurt, L. Gerland, H. Stöcker and M. Strikman, Phys. Rev **C64**, 054909 (2001).
20. R. Rapp and E.V. Shurayk, Phys. Lett. **B473**, 13 (2000).
21. WA98 Collaboration (M.M. Aggarwal *et al.*), Phys. Rev. Lett. **85**, 3593 (2000).
22. S.S. Adler *et al.*, PHENIX Collaboration, Phys. Rev. Lett. **91**, 072303 (2003).